International Journal of Thermal Sciences 49 (2010) 302–310

Contents lists available at ScienceDirect

International Journal of Thermal Sciences

journal homepage: www.elsevier.com/locate/ijts

Inverse radiation analysis in two-dimensional gray media using the discrete ordinates method with a multidimensional scheme

Carlos T. Salinas

Department of Mechanical Engineering, University of Taubaté, Rua Daniel Danelli s/n, Taubaté (SP) 12060-440, Brazil

ARTICLE INFO

Article history:
Received 2 February 2009
Received in revised form
10 August 2009
Accepted 18 August 2009
Available online 1 September 2009

Keywords:
Radiative transfer
Inverse radiation analysis
Conjugate gradient method
Temperature field
Discrete ordinates method

ABSTRACT

This work presents an inverse analysis for temperature field estimation in a two-dimensional gray media; it uses a multidimensional spatial scheme and high order angular quadrature in the discrete ordinates method. The participating media system contains absorbing, emitting, isotropic scattering gray medium. The radiative intensities exiting in some points of boundary surfaces, which simulate data of sensing devises, are known. In this work, the Discrete Ordinates Scheme with Infinitely Small Weight (DOS + ISW) is used to calculate data values. The conjugate gradient method is used to solve the inverse radiation problem for determining the temperature field. The inverse problem is formulated as an optimization problem that minimizes the error between the calculated and the simulated measurement of radiation intensity leaving the media that is sensed at one, two or four points at the boundary of the cavity. The numerical results are obtained by considering simulated data with and without noise. Different arrangements of the position of the sensors at the cavity boundary were analyzed. The temperature field has been estimated with accuracy by using LC11 and Tn6 angular quadratures of DOM when four or two sensors were used and the results for four and two sensors are very close. Also, the effects on the estimations of non-uniform distribution of the absorption coefficient (with random errors of 10%) were analyzed.

1. Introduction

Radiative heat transfer is the predominant mode of heat transfer in combustion chambers and furnaces. It is a very complicated phenomenon due to the gases that absorb, emit and scatter radiation. Since radiation affects the temperature field, accurate knowledge of the gas heat rate is required. In practice, two ways to predict the gas heat rate distribution are commonly used. The first one is to solve the theoretical combustion model or empirical formula that is not able to get an accurate result. The second one is to solve the inverse radiation problem.

The inverse analysis of radiation in participating medium has a broad range of engineering applications like the remote sensing of the atmosphere, determination of the radiative properties of medium, the prediction of flame temperature, the design of combustion systems such as furnaces, combustors and large-scale jet flames. Inverse radiation problems have been extensively reviewed in a series of papers by McCormick [1–4], by Howell and collaborators [5–7], and Ozisik and collaborators [8–10].

Direct radiation exchange problems are those in which radiative properties of the gases filling the enclosure as well as those of bounding surfaces along with boundary conditions are all known. These types of problems are mathematically "well posed"; therefore, they can be solved with straightforward and well-established mathematical procedures.

Inverse radiation exchange problems are, however, those in which some of the mentioned data are unknown but some additional information, such as measured or specified temperatures, are available. The inverse problem often leads to a mathematically ill-posed problem, because there may exist multiple solutions that satisfy the specified or desired conditions over the boundary surface or on the part of the domain, or no viable solution whatsoever. Consequently, standard analysis techniques will fail to produce a useful solution and special methods are required to treat the ill-formulated nature of equations.

Many researchers reported studies on inverse problems that deal with the prediction of the temperature distribution in a medium from either simulated or experimental radiation measurements (Li and Ozisik [8], Yi et al. [11], Siewert [12,13], Liu et al. [14,15], Li [16,17]). Most of the primary works considered one-dimensional systems, and assumed that the bounding surface was transparent or that the emissivity of the boundary surface was

E-mail address: csalinas_99@yahoo.com

1290-0729/$ – see front matter © 2009 Elsevier Masson SAS. All rights reserved.
doi:10.1016/j.ijthermalsci.2009.08.003

Nomenclature

$\boldsymbol{a}$	vector
$\boldsymbol{b}$	vector
$\boldsymbol{d}^k$	direction vector of descent in conjugate gradient method
dx, dy	dimensions of control volume in x and y direction (m)
$\boldsymbol{f}$	function
$\boldsymbol{g}$	function
$\boldsymbol{J}$	objective function
$\boldsymbol{I}$	radiation intensity (W m^{-2} sr^{-1})
$\boldsymbol{I}_b$	blackbody radiation intensity (W m^{-2} sr^{-1})
M	number of discrete directions
M, N	Polynomial order
$\overline{n}$	refractive index
$\boldsymbol{Q}$	dimensionless heat flux
$\boldsymbol{q}$	local heat flux per unit area (W m^{-2})
$\boldsymbol{q_r}$	net total radiative flux (W m^{-2})
$\boldsymbol{r}$	vector position (m)
S_r	radiative source term (W m^{-3})
S	source term (W m^{-3})
T	temperature (K)
$\boldsymbol{w}$	weight of angular quadrature
$\boldsymbol{x}$	vector
x_L, y_L	dimensions of the cavity in x and y direction (m)
x/y	x/y-coordinate (m)
$\boldsymbol{Y}$	measured exit radiation intensities (W m^{-2} sr^{-1})

Greek symbol

α	step size
β	extinction coefficient (m^{-1})
β_0	conjugate coefficient
δ^*	small specified positive number
ε	total emissivity
κ	absorption coefficient (m^{-1})
ρ	reflectivity
σ	scattering coefficient (m^{-1})
σ_o	standard deviation
$\overline{\sigma}$	Stefan Boltzmann constant (W m^{-2} K^{-4})
μ	direction cosine
ξ	direction cosine
Ω	direction vector
ω	single scattering albedo
∇	gradiente

Subscripts

i,j	space grid position
m	the mth discrete ordinate

Superscripts

k	iteration number
n	iteration number
m	the mth discrete ordinate

known. Li and Ozisik [9], Liu et al. [18] reconstructed simultaneously temperature profiles and wall emissivity in parallel plane media. Neto and Ozisik [10] simultaneously estimated the optical thickness, the albedo and the scattering phase function in a parallel plane media. Li [19] studied the inverse problem of an unknown source term in a two-dimensional rectangular medium with transparent boundaries. Zhou et al. [20] used an optimization procedure for estimating simultaneously the temperature and scattering albedo profiles.

In most of the above works, the discrete ordinates method (DOM), the discrete transfer method (DTM), the zonal method or the Monte Carlo method were employed to solve the direct and the sensitivity problems.

For a system governed by radiation, the inverse problem is represented by a set of Fredholm equations of the first type that are known to be ill-posed. Regularization is needed to allow recovering an acceptable solution for an inverse problem whose exact solution is completely corrupted by the noisy data.

There exist a number of regularized solution techniques that have been used for solving similar problems, including truncated singular value decomposition (TSVD) [6], the conjugate gradient method (CGM) [21], the bi-conjugate gradient method (BiCGM) that is a method based on the CGM and improves the method to solve any arbitrary MxN system [5] and the Tikhonov regularization method that was first proposed by Tikhonov [22] for solving inverse conduction problems. Reviews of regularization methods were provided by Björck [23], Hansen [24], Vogel [25] and Daun and Howell [7].

Despite the relatively large interest expressed in inverse radiation problems of temperature distributions in media, most of the works use simple spatial interpolation schemes like the step and diamond scheme, and a low order of angular quadratures for the discrete ordinates method (DOM). Less accurate solutions were used for the direct problems.

The inverse radiation problem considered in this paper is concerned with the estimation of the source term distribution or temperature profile in 2-D participating media systems containing absorbing, emitting and scattering gray medium from knowing the radiative intensities exiting in some points of boundary surfaces that simulate dates received by sensing devises. In practical experimental measurements of radiation intensity at a point (in fact, a pinhole) of the boundary of some domain, it is possible to obtain a set of directional intensities in 180, 240 or more directions for 2-D calculations in a cross section depending on the resolution of the sensor in the experimental device. Then it is possible to select different angular quadratures that can be adjusted to the experimental data. Based on this, different angular quadratures for DOM and a different number of sensors are used in this numerical study to examine the effects of these on the accuracy of the estimation.

The inverse problem is formulated as an optimization problem and the conjugate gradient method is used for its solution. In this work, the discrete ordinates method is used to solve the direct and the sensitivity problems. A multidimensional high order spatial scheme and different angular quadratures for the discrete ordinates method are used to examine the accuracy of the estimation. Analysis is made of the direct problem, the gradient equation and the sensitivity problem. The procedure for each of these steps is described and then an algorithm for the solution of the inverse radiation problem is presented. Finally, several inverse problems of the source term in two-dimensions are investigated to demonstrate the computational accuracy and efficiency of the inverse analysis method presented in this paper.

2. Analysis

The analysis consists of the direct problem, the gradient equation, and the sensitivity problem.

2.1. Direct problem

It considers the radiative transfer process in an absorbing, emitting, scattering, gray and two-dimensional rectangular medium (see Fig. 1). The boundary surfaces are considered to be transparent. There is no external incident radiation. The radiative properties, such as single scattering albedo ω absorption coefficient of the medium, are assumed to be uniform everywhere. The direct problem of concern here is to find the exiting radiative intensities at the boundaries for the known source term distribution and radiative properties.

The radiative transport equation for an absorbing, emitting gray gas with isotropic scattering can be written as Siegel and Howell [26] did,

$$(\Omega.\nabla)\boldsymbol{I}(\boldsymbol{r},\Omega) = -(\kappa+\sigma)\boldsymbol{I}(\boldsymbol{r},\Omega) + S(\boldsymbol{r}) + \frac{\sigma}{4\pi}\int_{4\pi}\boldsymbol{I}(\boldsymbol{r},\Omega')\boldsymbol{d}\Omega' \quad (1)$$

where $\boldsymbol{I}(\boldsymbol{r},\Omega)$ is the radiation intensity in $\boldsymbol{r}$, and in the direction Ω; $\boldsymbol{I}_b(\boldsymbol{r})$, is the radiation intensity of the blackbody in position $\boldsymbol{r}$ and at the temperature of the medium; κ is the gray medium absorption coefficient; σ is the gray medium scatter coefficient; and the integration is in the incident direction Ω'. The source term $S(\boldsymbol{r})$ is related to the temperature $T(\boldsymbol{r})$ of the medium by

$$S(\boldsymbol{r}) = \frac{(1-\omega)\overline{n}^2\overline{\sigma}\boldsymbol{T}^4(\boldsymbol{r})}{\pi} \quad (2)$$

Here, $\overline{n}$ is the refractive index and $\overline{\sigma}$ is the Stefan Boltzmann constant.

For diffusely reflecting surfaces the radiative boundary condition for Eq. (1) is

$$\boldsymbol{I}(\boldsymbol{r},\Omega) = \epsilon\boldsymbol{I}_b(\boldsymbol{r}) + \frac{\rho}{\pi}\int_{\boldsymbol{n}\cdot\Omega'<0}|\boldsymbol{n}\cdot\Omega'|\boldsymbol{I}(\boldsymbol{r},\Omega')\boldsymbol{d}\Omega' \quad (3)$$

where $\boldsymbol{r}$ lies on the boundary surface Γ, and Eq. (3) is valid for $\boldsymbol{n}\cdot\Omega > 0$. $\boldsymbol{I}(\boldsymbol{r},\Omega)$ is the radiation intensity leaving the surface at the boundary condition, ϵ is the surface emissivity, ρ is the surface reflectivity and $\boldsymbol{n}$ is the unit vector normal to the boundary surface.

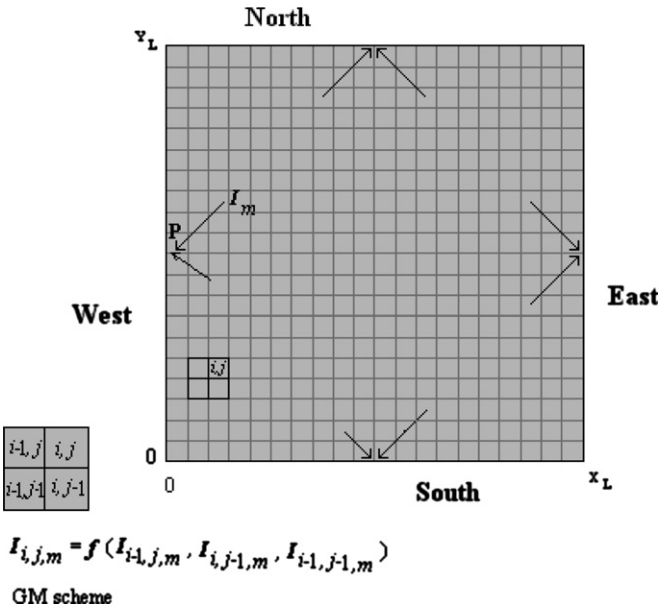

Fig. 1. Scheme of physical system and mesh cell in two-dimensional rectangular geometry.

In the method of discrete ordinates, the equation of radiation transport is substituted by a set of M discrete equations for a finite number of directions Ω_m, and each integral is substituted by a quadrature series [27],

$$(\Omega_m\cdot\nabla)\boldsymbol{I}(\boldsymbol{r},\Omega_m) = -\beta\boldsymbol{I}(\boldsymbol{r},\Omega_m) + \boldsymbol{S}(\boldsymbol{r}) + \frac{\sigma}{4\pi}\sum_{m=1}^{M}\boldsymbol{w}_m\boldsymbol{I}(\boldsymbol{r},\Omega_m) \quad (4)$$

This angular approximation transforms the original equation into a set of coupled differential equations with $\beta = (\kappa+\sigma)$ as the extinction coefficient.

$$\boldsymbol{S}_m = \frac{\sigma}{4\pi}\sum_{m=1}^{M}\boldsymbol{w}_m\boldsymbol{I}(\boldsymbol{r},\Omega_m) \quad (5)$$

where $\boldsymbol{S}_m$ represents the entering scattering source term, $\boldsymbol{w}_m$ are the ordinates weight, M is the number of directions Ω_{m} of the angular quadrature and $\boldsymbol{I}_m$ is obtained by solving the radiative transport equation in discrete ordinates.

In the Cartesian ordinate system the two-dimensional radiative transport equation in the m direction for an emitting, absorbing and scattering medium is

$$\mu_m\frac{\boldsymbol{dI}_m}{\boldsymbol{dx}} + \xi_m\frac{\boldsymbol{dI}_m}{\boldsymbol{dy}} = \beta\boldsymbol{I}_m + \boldsymbol{S}(x,y) + \boldsymbol{S}_m \quad (6)$$

where μ_m, ξ_m, are the directional cosine of Ω_m. The boundary condition in discrete ordinates for the case analyzed in this work can be written as

$$\boldsymbol{I}_m = 0; \quad \mu_m > 0 \text{ in } x = 0 \quad (7a)$$

$$\boldsymbol{I}_m = 0; \quad \mu_m < 0 \text{ in } x = x_L \quad (7b)$$

$$\boldsymbol{I}_m = 0; \quad \xi_m > 0 \text{ in } y = 0 \quad (7c)$$

$$\boldsymbol{I}_m = 0; \quad \xi_m < 0 \text{ in } y = y_L \quad (7d)$$

The direct problem is solved using the numerical method outlined in Ismail and Salinas [28]. The multidimensional non-linear high order scheme of Balsara [29], the so-called genuinely multidimensional (GM) is used here in the spatial discretization. Validation of the model and numerical method used for the direct problem can be found in [28].

2.2. Inverse problem

For the inverse problem, the source term distribution or the temperature distribution are unknown, but the other quantities in Eq. (6) and Eqs. (7) are known. Measured exit radiative intensities in a point on every one of the four wall boundaries or two opposite wall boundaries or a single point in one wall boundary of the cavity are considered available. In the inverse analysis, the source term distribution is estimated by the measured data of exit radiative intensities.

The source term can be represented by a polynomial as

$$\boldsymbol{S}(x,y) = \sum_{q=0}^{M}\sum_{r=0}^{N}\boldsymbol{a}_{qr}\boldsymbol{f}_q(x)\boldsymbol{g}_r(y) \quad (8)$$

where $\boldsymbol{f}_q(x)$ e $\boldsymbol{g}_r(y)$ are basic functions, M and N is the order of the source term polynomial expansion.

The inverse radiation problem can be formulated as an optimization problem. In the case of one measurement point at the center of every wall of a square cavity, we wish to minimize the objective function:

$$\begin{aligned}\boldsymbol{J}(\tilde{\boldsymbol{a}}) = & \sum_{\mu_i<0} \boldsymbol{w}_i[\boldsymbol{I}_1(x_0, 0.5y_L, \mu_i, \tilde{\boldsymbol{a}}) \\ & - \boldsymbol{Y}_1(\mu_i)]^2 + \sum_{\mu_i>0} \boldsymbol{w}_i[\boldsymbol{I}_2(x_L, 0.5y_L, \mu_i, \tilde{\boldsymbol{a}}) \\ & - \boldsymbol{Y}_2(\mu_i)]^2 + \sum_{\xi_i<0} \boldsymbol{w}_i[\boldsymbol{I}_3(0.5x_L, y_0, \xi_i, \tilde{\boldsymbol{a}}) \\ & - \boldsymbol{Y}_3(\xi_i)]^2 + \sum_{\xi_i>0} \boldsymbol{w}_i[\boldsymbol{I}_4(0.5x_L, y_L, \xi_i, \tilde{\boldsymbol{a}}) - \boldsymbol{Y}_4(\xi_i)]^2 \end{aligned} \tag{9.a}$$

where $\boldsymbol{Y}_1(\mu_i)$, $\boldsymbol{Y}_2(\mu_i)$, $\boldsymbol{Y}_3(\xi_i)$ and $\boldsymbol{Y}_4(\xi_i)$ are measured exit radiation intensities at the boundaries in the points (x, y): $(x_0, y_L/2)$, $(x_L, y_L/2)$, $(x_L/2, y_0)$ and $(x_L/2, y_L)$ respectively, where $x_0 = 0$ and $y_0 = 0$; $\boldsymbol{I}_1, \boldsymbol{I}_2, \boldsymbol{I}_3$ e $\boldsymbol{I}_4$, are estimated exit radiation intensities at $(x_0, y_L/2)$, $(x_L, y_L/2)$, $(x_L/2, y_0)$ and $(x_L/2, y_L)$, respectively, for the estimated vector $\tilde{\boldsymbol{a}} = (a_{00}, a_{10}, \ldots, a_{MN})^T$.

In the case of one measurement point at the center of two appositive vertical walls of a square cavity, we wish to minimize the objective function:

$$\begin{aligned}\boldsymbol{J}(\tilde{\boldsymbol{a}}) = & \sum_{\mu_i<0} \boldsymbol{w}_i[\boldsymbol{I}_1(x_0, 0.5y_L, \mu_i, \tilde{\boldsymbol{a}}) \\ & - \boldsymbol{Y}_1(\mu_i)]^2 + \sum_{\mu_i>0} \boldsymbol{w}_i[\boldsymbol{I}_2(x_L, 0.5y_L, \mu_i, \tilde{\boldsymbol{a}}) - \boldsymbol{Y}_2(\mu_i)]^2 \end{aligned} \tag{9.b}$$

In the case of one measurement point at the center of west wall of a square cavity, we wish to minimize the objective function:

$$\boldsymbol{J}(\tilde{\boldsymbol{a}}) = \sum_{\mu_i<0} \boldsymbol{w}_i[\boldsymbol{I}_1(x_0, 0.5y_L, \mu_i, \tilde{\boldsymbol{a}}) - \boldsymbol{Y}_1(\mu_i)]^2 \tag{9.c}$$

If a single point is selected in any other wall of the square cavity, similar proper objective function can be used in Eq. (9.c).

Other measurement points different than the wall center points can be used, but in these cases the points need to be considered in Eq. (9.a) or Eq. (9.b) or Eq. (9.c) and in the calculation of the $\boldsymbol{I}_i$ and $\boldsymbol{Y}_i$ values.

In all the above cases, the problem is to find the vector $\tilde{\boldsymbol{a}}$ that minimizes the function $\boldsymbol{J}$.

The computational algorithm of this minimization procedure consists of two main modules: the direct radiation computation and the search modules. As explained previously, for the first module the Discrete Ordinates Method (DOM) with the multidimensional spatial scheme is employed in this work, while for the latter the Conjugate Gradient Method (CGM) is used as the basic search method to minimize the function $\boldsymbol{J}$.

2.3. Conjugate gradient method of minimization

The minimization of the objective function with respect to the desired vector is the most important procedure in solving the inverse problem. The Conjugate Gradient Method for determining unknown temperature distribution is used in this work. The derivation of the method is presented in Hansen [24] and Beckman [30] in detail.

Iterations are built in the following manner [8,15]:

$$\boldsymbol{a}^{k+1} = \boldsymbol{a}^k - \alpha^k \boldsymbol{d}^k \tag{10}$$

where α^k is the step size, $\boldsymbol{d}^k$ is the direction vector of descent given by

$$\boldsymbol{d}^k + \nabla \boldsymbol{J}(\boldsymbol{a}^k) + \beta_0^k \boldsymbol{d}^{k-1} \tag{11}$$

and the conjugate coefficient β^k is determined from

$$\beta_0^k = \frac{\nabla \boldsymbol{J}(\boldsymbol{a}^k) \nabla \boldsymbol{J}^T(\boldsymbol{a}^k)}{\nabla J(\boldsymbol{a}^{k-1}) \nabla \boldsymbol{J}^T(\boldsymbol{a}^{k-1})} \quad \beta_0^0 = 0 \tag{12}$$

where the row vector $\nabla \boldsymbol{J}$ defined by

$$\nabla \boldsymbol{J} = \left(\frac{\partial \boldsymbol{J}}{\partial \boldsymbol{a}_{00}}, \frac{\partial \boldsymbol{J}}{\partial \boldsymbol{a}_{10}}, \ldots\ldots, \frac{\partial \boldsymbol{J}}{\partial \boldsymbol{a}_{MN}} \right) \tag{13}$$

is the gradient of the objective function. For four measurement points, its components are defined as

$$\begin{aligned}\frac{\partial \boldsymbol{J}(\tilde{\boldsymbol{a}})}{\partial \boldsymbol{a}_{qr}} = & 2 \sum_{\mu_i<0} \boldsymbol{w}_i[\boldsymbol{I}_1(x_0, 0.5y_L, \mu_i, \tilde{\boldsymbol{a}}) \\ & - \boldsymbol{Y}_1(\mu_i)] \frac{\partial \boldsymbol{I}_1(x_0, 0.5y_L, \mu_i, \tilde{\boldsymbol{a}})}{\partial \boldsymbol{a}_{qr}} + 2 \\ & \times \sum_{\mu_i>0} \boldsymbol{w}_i[\boldsymbol{I}_2(x_L, 0.5y_L, \mu_i, \tilde{\boldsymbol{a}}) \\ & - \boldsymbol{Y}_2(\mu_i)] \frac{\partial \boldsymbol{I}_2(x_L, 0.5y_L, \mu_i, \tilde{\boldsymbol{a}})}{\partial \boldsymbol{a}_{qr}} + 2 \\ & \times \sum_{\xi_i<0} \boldsymbol{w}_i[\boldsymbol{I}_3(0.5x_L, y_0, \xi_i, \tilde{\boldsymbol{a}}) \\ & - \boldsymbol{Y}_3(\xi_i)] \frac{\partial \boldsymbol{I}_3(0.5x_L, y_0, \xi_i, \tilde{\boldsymbol{a}})}{\partial \boldsymbol{a}_{qr}} + 2 \\ & \times \sum_{\xi_i>0} \boldsymbol{w}_i[\boldsymbol{I}_4(0.5x_L, y_L, \xi_i, \tilde{\boldsymbol{a}}) \\ & - \boldsymbol{Y}_4(\xi_i)] \frac{\partial \boldsymbol{I}_4(0.5x_L, y_L, \xi_i, \tilde{\boldsymbol{a}})}{\partial \boldsymbol{a}_{qr}} \end{aligned} \tag{14.a}$$

For two measurement points, its components are defined as

$$\begin{aligned}\frac{\partial \boldsymbol{J}(\tilde{\boldsymbol{a}})}{\partial \boldsymbol{a}_{qr}} = & 2 \sum_{\mu_i<0} \boldsymbol{w}_i[\boldsymbol{I}_1(x_0, 0.5y_L, \mu_i, \tilde{\boldsymbol{a}}) \\ & - \boldsymbol{Y}_1(\mu_i)] \frac{\partial \boldsymbol{I}_1(x_0, 0.5y_L, \mu_i, \tilde{\boldsymbol{a}})}{\partial \boldsymbol{a}_{qr}} + 2 \\ & \sum_{\mu_i>0} \boldsymbol{w}_i[\boldsymbol{I}_2(x_L, 0.5y_L, \mu_i, \tilde{\boldsymbol{a}}) \\ & - \boldsymbol{Y}_2(\mu_i)] \frac{\partial \boldsymbol{I}_2(x_L, 0.5y_L, \mu_i, \tilde{\boldsymbol{a}})}{\partial \boldsymbol{a}_{qr}} \end{aligned} \tag{14.b}$$

In principle, the step size of the k th iteration α^k can be determined by minimizing the function, $\boldsymbol{J}(\boldsymbol{a}^k - \alpha^k \boldsymbol{d}^k)$, for the given $\boldsymbol{a}^k$ and $\boldsymbol{d}^k$ in the following manner:

$$\frac{\partial \boldsymbol{J}(\boldsymbol{a}^k - \alpha^k \boldsymbol{d}^k)}{\partial \alpha^k} = 0 \tag{15}$$

Since $\boldsymbol{J}(\mathbf{a}^k - \alpha^k \mathbf{d}^k)$ is the implicit function of α^k, the exact step is difficult to solve. We make the first-order Taylor expansion of the function with respect to α^k.

For four measurement points, using Eq. (15), we have in discrete ordinates

$$\alpha^k = \Bigg\{ \sum_{\mu_i<0} \boldsymbol{w}_i[\boldsymbol{I}_1(x_0, 0.5y_L, \mu_i, \tilde{\boldsymbol{a}}^k) - \boldsymbol{Y}_1(\mu_i)] \times [\nabla \boldsymbol{I}_1(x_0, 0.5y_L, \mu_i, \tilde{\boldsymbol{a}}^k)\boldsymbol{d}^k] + \sum_{\mu_i>0} \boldsymbol{w}_i[\boldsymbol{I}_2(x_L, 0.5y_L, \mu_i, \tilde{\boldsymbol{a}}^k) - \boldsymbol{Y}_2(\mu_i)][\nabla \boldsymbol{I}_2(x_L, 0.5y_L, \mu_i, \tilde{\boldsymbol{a}}^k)\boldsymbol{d}^k] + \sum_{\xi_i<0} \boldsymbol{w}_i[\boldsymbol{I}_3(0.5x_L, y_0, \xi_i, \tilde{\boldsymbol{a}}^k) - \boldsymbol{Y}_3(\xi_i)] \times [\nabla \boldsymbol{I}_3(0.5x_L, y_0, \xi_i, \tilde{\boldsymbol{a}}^k)\boldsymbol{d}^k] + \sum_{\xi_i>0} \boldsymbol{w}_i[\boldsymbol{I}_4(0.5x_L, y_L, \xi_i, \tilde{\boldsymbol{a}}^k) - \boldsymbol{Y}_4(\xi_i)][\nabla \boldsymbol{I}_4(0.5x_L, y_L, \xi_i, \tilde{\boldsymbol{a}}^k)\boldsymbol{d}^k] \Bigg\} \Bigg/ \Bigg\{ \sum_{\mu_i<0} \boldsymbol{w}_i[\nabla \boldsymbol{I}_1(x_0, 0.5y_{L,}\mu_i, \tilde{\boldsymbol{a}}^k)\boldsymbol{d}^k]^2 + \sum_{\mu_i>0} \boldsymbol{w}_i[\nabla \boldsymbol{I}_2(x_L, 0.5y_L, \mu_i, \tilde{\boldsymbol{a}}^k)\boldsymbol{d}^k]^2 + \sum_{\xi_i<0} \boldsymbol{w}_i[\nabla \boldsymbol{I}_3(0.5x_L, y_{0,}\xi_i, \tilde{\boldsymbol{a}}^k)\boldsymbol{d}^k]^2 + \sum_{\xi_i>0} \boldsymbol{w}_i[\nabla \boldsymbol{I}_4(0.5x_L, y_L, \xi_i, \tilde{\boldsymbol{a}}^k)\boldsymbol{d}^k]^2 \Bigg\} \tag{16.a}$$

For two measurement points, we have in discrete ordinates

$$\alpha^k = \Bigg\{ \sum_{\mu_i<0} \boldsymbol{w}_i[\boldsymbol{I}_1(x_0, 0.5y_L, \mu_i, \tilde{\boldsymbol{a}}^k) - \boldsymbol{Y}_1(\mu_i)] \times [\nabla \boldsymbol{I}_1(x_0, 0.5y_L, \mu_i, \tilde{\boldsymbol{a}}^k)\boldsymbol{d}^k] + \sum_{\mu_i>0} \boldsymbol{w}_i[\boldsymbol{I}_2(x_L, 0.5y_L, \mu_i, \tilde{\boldsymbol{a}}^k) - \boldsymbol{Y}_2(\mu_i)][\nabla \boldsymbol{I}_2(x_L, 0.5y_L, \mu_i, \tilde{\boldsymbol{a}}^k)\boldsymbol{d}^k] \Bigg\} \Bigg/ \Bigg\{ \sum_{\mu_i<0} \boldsymbol{w}_i[\nabla \boldsymbol{I}_1(x_0, 0.5y_{L,}\mu_i, \tilde{\boldsymbol{a}}^k)\boldsymbol{d}^k]^2 + \sum_{\mu_i>0} \boldsymbol{w}_i[\nabla \boldsymbol{I}_2(x_L, 0.5y_L, \mu_i, \tilde{\boldsymbol{a}}^k)\boldsymbol{d}^k]^2 \Bigg\} \tag{16.b}$$

where the row vector

$$\nabla \boldsymbol{I} = \left(\frac{\partial \boldsymbol{I}}{\partial \boldsymbol{a}_{00}}, \frac{\partial \boldsymbol{I}}{\partial \boldsymbol{a}_1 0}, \cdots\cdots\cdots, \frac{\partial \boldsymbol{I}}{\partial \boldsymbol{a}_{\mathrm{MN}}} \right) \tag{17}$$

is the sensitivity coefficient vector, which is essential in the solution procedure of the inverse problem.

2.4. Sensitivity problem

To obtain the sensitivity coefficients, we substitute Eq. (8) into Eq. (6) and differentiate the direct problem defined by Eqs. (6) and (7) with respect to $\boldsymbol{a}_{qr}$. The equations of sensitivity coefficients can be written as

$$\mu \frac{\partial}{\partial x}\left(\frac{\partial \boldsymbol{I}(x,y,\Omega)}{\partial \boldsymbol{a}_{qr}} \right) + \xi \frac{\partial}{\partial y}\left(\frac{\partial \boldsymbol{I}(x,y,\Omega)}{\partial \boldsymbol{a}_{qr}} \right) + \beta \left(\frac{\partial \boldsymbol{I}(x,y,\Omega)}{\partial \boldsymbol{a}_{qr}} \right) = \boldsymbol{f}_q(x)\boldsymbol{g}_r(y) + \frac{\omega}{4\pi} \int_{4\pi} \frac{\partial \boldsymbol{I}(x,y,\Omega')}{\partial \boldsymbol{a}_{qr}} d\Omega' \tag{18}$$

where $q = 1, 2, \ldots\ldots, M$ and $r = 1, 2, \ldots\ldots, N$

With the boundary conditions

$$\left(\frac{\partial I(x,y,\Omega)}{\partial a_{qr}} \right) = 0 \; x = 0, \mu > 0; \; \left(\frac{\partial I(x,y,\Omega)}{\partial a_{qr}} \right) = 0 \; x = x_L, \mu < 0$$
$$\left(\frac{\partial I(x,y,\Omega)}{\partial a_{qr}} \right) = 0 \; y = 0, \xi > 0; \; \left(\frac{\partial I(x,y,\Omega)}{\partial a_{qr}} \right) = 0 \; y = y_L, \xi < 0 \tag{19}$$

A similar numerical iteration procedure as the direct problem is used for the solution of the sensitivity problem. Because the sensitivity coefficient vector $\nabla \boldsymbol{I}$ is independent of the vector $\boldsymbol{a}$, the estimation of the source term distribution is linear, and it is only necessary to solve it once at first.

2.5. Stopping criterion and error estimation

The stopping criterion of the iteration is selected in the following manner: if the problem contains no measurement error, the following condition

$$\boldsymbol{J}(\boldsymbol{a}^{k+1}) < \delta^* \tag{20}$$

is used for terminating the iterative process, where δ^* is a small specified positive number; otherwise, it is used in the following two conditions

$$\boldsymbol{J}(\boldsymbol{a}^k) - \boldsymbol{J}(\boldsymbol{a}^{k+1}) < \delta_1^* \tag{21}$$

where δ_1^* is a small specified positive number, and the discrepancy principle [19,31]

$$\boldsymbol{J}(\boldsymbol{a}^{k+1}) = 8\pi\sigma_0^2 \tag{22}$$

where σ_o is the standard deviation. For four measurement points, it is written in discrete ordinates as

$$\boldsymbol{J}(\boldsymbol{a}^{k+1}) < \sum_{\mu_m<0} \sigma_{0W,m}^2 + \sum_{\mu_m>0} \sigma_{0E,m}^2 + \sum_{\xi_m<0} \sigma_{0S,m}^2 + \sum_{\xi>0} \sigma_{0N,m}^2 \tag{23.a}$$

For two measurement points, it is written in discrete ordinates as

$$\boldsymbol{J}(\boldsymbol{a}^{k+1}) < \sum_{\mu_m<0} \sigma_{0W,m}^2 + \sum_{\mu_m>0} \sigma_{0E,m}^2 \tag{23.b}$$

When Eq. (21) or Eqs. (23) is satisfied, then it is used as the stopping criterion. After several numerical experiments, the value of δ_1^* is selected as 10^{-5}.

To examine the accuracy of the estimation by using the multi-dimensional spatial scheme and high order angular quadratures for DOM, the relative error and the rms error defined as [19] will be used.

$$\text{Relative error} = \frac{\boldsymbol{S}_{\text{estimated}}(x,y) - \boldsymbol{S}_{\text{exact}}(x,y)}{\boldsymbol{S}_{\text{exact}}(x,y)} \tag{24}$$

$$\text{rms error} = \left\{ \frac{1}{x_L y_L} \int_0^{y_L} \int_0^{x_L} [\boldsymbol{S}_{\text{estimated}}(x,y) - \boldsymbol{S}_{exact}(x,y)]^2 dx dy \right\}^{1/2} \tag{25}$$

The computational algorithm for the solution of the inverse radiation problem follows the method outlined in [8,19].

3. Results and discussion

Based on the theoretical and numerical analysis described earlier, a computer code has been developed to solve the inverse radiation problem of the source term in two-dimensional rectangular media by knowing the exit radiation at points in different positions on the boundaries. To examine the accuracy of the method presented in this paper, two different test cases are considered. In the first case, four measurement points are considered and assuming the measurement data exit radiation intensities have errors or do not have errors, the temperature profile is determined. Different angular quadratures of DOM are tested and their accuracy on the estimation is presented. In the second case, the effects of the number of measurement points and their positions on the estimation are analyzed. Results for one, two and four measurement points are compared. The optical thickness of the slab is chosen to be 1.0. To simulate the measured exit radiation intensities, $\boldsymbol{Y}_i$, containing measurement errors, random errors of standard deviation σ_o are added to the exact exit radiation intensities computed from the solution of the direct problem. Thus we have

$$(\boldsymbol{Y}_i)_{\text{measured}} = (\boldsymbol{Y}_i)_{\text{exact}} + \sigma_0\ \zeta \quad i = 1,2,3,4 \tag{26}$$

where ζ is a normal distribution random variable with a zero mean and unit standard deviation. There is a 99% probability of ζ lying in the range $-2.567 < \zeta < 2.567$ [8]. For all the results presented in this work, it is assumed that the exit radiation intensities are available at the quadrature points for Sn [29], LC11 [32] and Tn [33] angular quadratures of DOM. In this work, the Discrete Ordinates Scheme with Infinitely Small Weight (DOS + ISW) [34] is used to calculate the $(\boldsymbol{Y}_i)_{\text{exact}}$ values. In that method, one or more new discrete directions are added to an existing discrete ordinate quadrature set, and weights associated with these new directions are set infinitely small. The new discrete direction(s) and the original quadrature set make up a new discrete ordinate quadrature set. The $(\boldsymbol{Y}_i)_{\text{exact}}$ values are calculated using the $(\text{ISW}_{S4} + \text{ISW}_{S6} + \text{ISW}_{LC11}) + \text{Tn6}$ angular quadrature.

First we consider a source term expressed as a polynomial of degree 4 as in [19],

$$S(x,y) = 1 + 6x + 3y + 4x^2 + 2y^2 + 5x^4y^4,\ W/m^2 \tag{27}$$

The estimated values of the source term by inverse analysis are calculated. Fig. 2 shows the characteristic convergence of the objective function $\boldsymbol{J}$ for the solution of the inverse problem for σ_o equal to 0.0 and 0.12. For σ_o equal to 0.0, the value of δ^* in Eq. (20) is selected after a series of numerical experiments using the graphics of convergence. For σ_o equal to 0.12, as can be see in Fig. 2(b), the function objective decreases faster in the first iterations until it reaches some value that sometimes is a little higher than the stopping criterion value of Eq. (23), and then converges slowly. In these cases the stopping criterion given by Eq. (21) help to finish the iterations. The value of δ_1^* in Eq. (21) is selected being equal to 10^{-5} after several numerical experiments using the graphics of convergence.

With no measurement errors, $\sigma_o = 0$, no observable difference was detected between the exact values of the source term and the estimated values when the LC11 angular quadrature is used. Otherwise, when the quadrature S_6 is used, discrepancies are observed with the exact solution. To show the accuracy of the estimation more clearly, the heat flux on the west wall for different angular quadratures is shown in Fig. 3. This heat flux is calculated using the estimated source term. It can be observed that the estimation of heat flux on the west wall agrees well with the heat flux calculated when using the exact solution with the LC11 quadrature;

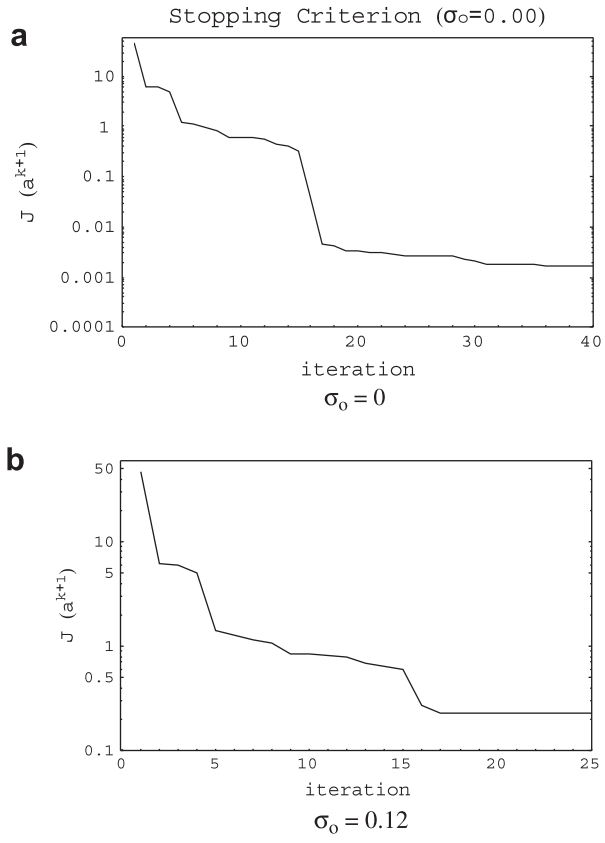

Fig. 2. Characteristic convergence profile of the function objective.

a poor estimation is found when Sn6 quadrature is used. The accuracy of the estimation is sensitive to the angular quadratures used. Estimations when the Tn6 quadrature is used is as accurate as an estimation with LC11 quadrature and is not presented in Fig. 3 for the sake of graphic clarity because the points seem to be the same.

In the practical process of measurement and inverse solution, the measured parameters may have random errors. In order to examine the effect of these errors on temperature estimation, it is assumed that the simulated experimental data contain random measurement errors of standard deviation $\sigma_o = 0.03$, $\sigma_o = 0.06$ and $\sigma_o = 0.12$. Different sets of random numbers were used for simulating measurements in each boundary and different sets of

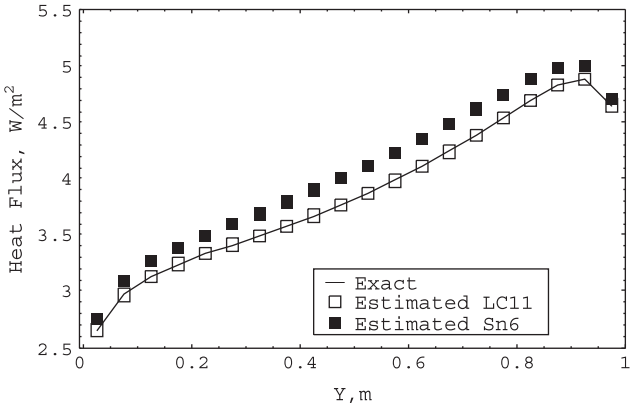

Fig. 3. Estimation of the heat flux on west wall using simulated measured exit radiation intensity data with $\sigma_o = 0$ and different angular quadratures of DOM.

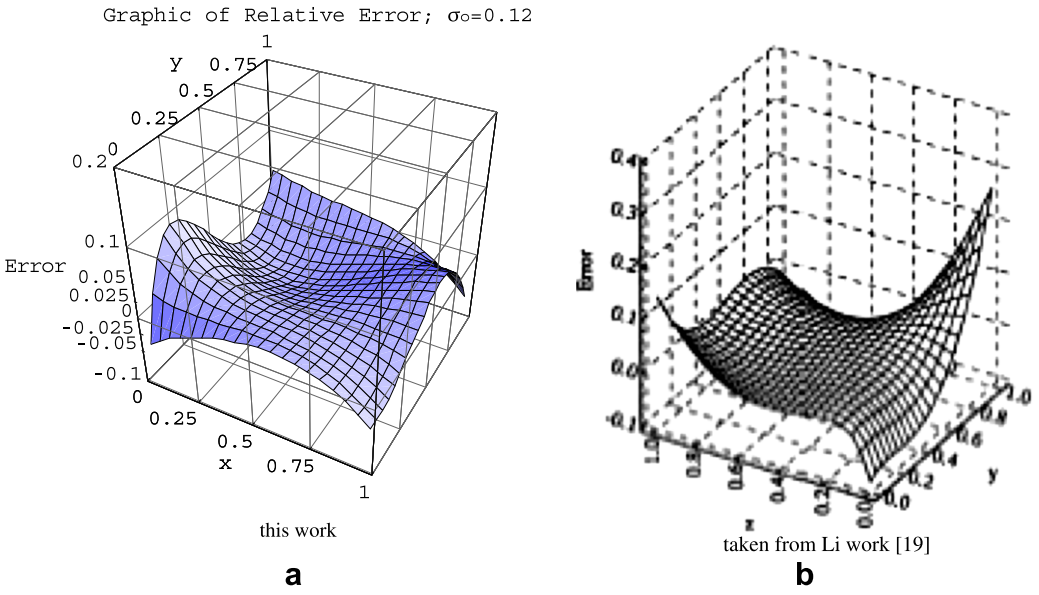

Fig. 4. Comparison of the relative error for $\sigma_o = 0.12$.

random numbers were used to repeat the inverse calculations. To show the accuracy of the estimation more clearly, the relative error defined in Eq. (24) is calculated and the results are compared with existing results reported in [19]. Fig. 4(a) shows the relative error of the estimation in this work for σ_o equal to 0.12 and it is compared with the results in Fig. 4(b) taken from the Li work [19]. Substantially less relative error in our result can be observed (maximum error of 8.8% compared with 26.7% in [19]) and this shows that the use of the multidimensional spatial scheme and high order angular quadrature for DOM permit a more accurate estimation.

To show the accuracy of the estimation more clearly, the heat flux on the west wall for σ_o equal to 0.03, 0.06 and 0.12 is shown in Fig. 5. This heat flux is calculated using the estimated source term. All the estimations in this figure are for the LC11 quadrature. Clearly, the agreement between the exact and the estimated results for the heat flux on the west wall is good for σ_o equal to 0.03 and 0.06. The accuracy decreases when a strong noise with σ_o equal to 0.12 is used, but the results still have good approximation.

To examine the effects of the number of measurement points on the estimation several numerical experiments were realized. Fig. 6 shows the comparison of the estimations using simulated measured exit radiation intensity data in one, two and four measurement points. A strong noise of σ_o equal to 0.12 and center wall measurement points was used in these estimations. Fig. 6(a) shows the estimations of the radiative dissipation source at $y = 0.5$

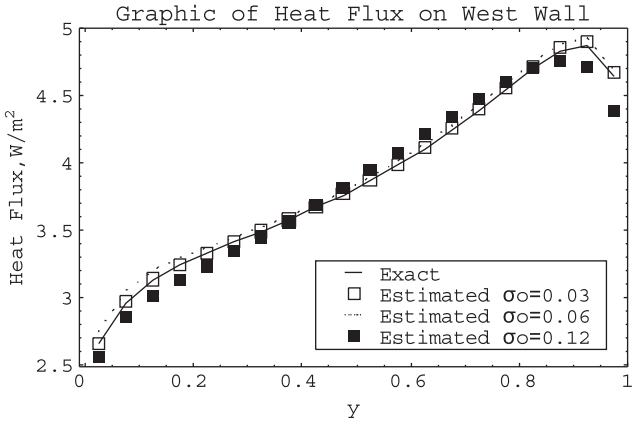

Fig. 5. Comparison of the estimation of the heat flux using simulated measured exit radiation intensity data with angular quadratures LC11, for $\sigma_o = 0.03$, 0.06 and 0.12.

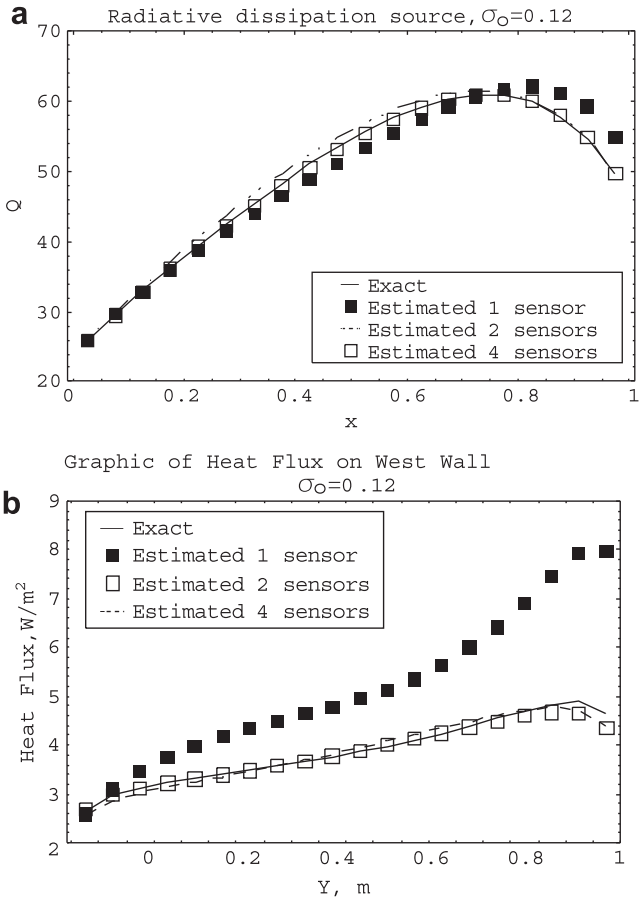

Fig. 6. Comparison of the estimation using simulated measured exit radiation intensity data in one, two and four measurement points, for $\sigma_o = 0.12$.

Table 1
RMS error of the estimation for the source term $S(x,y)$, with isotropic scattering, $\omega = 0.5$, $x_L = y_L = 1$.

σ_o	RMS (2 sensors)	RMS (4 sensors)	RMS (4 sensors)
	This work	This work	Li work [19]
0	0.000	0.000	0.000
0.06	0.126	0.079	0.212
0.12	0.229	0.149	0.248

Table 2
RMS error of the estimation for the source term $\boldsymbol{S}(x,y)$, with isotropic scattering, $\omega = 0.5$, $x_L = y_L = 1$ and 10% error on the absorption coefficient.

σ_o	RMS (2 sensors)	RMS (2 sensors)	RMS (4 sensors)
	κ uniform	κ non-uniform	Li work [19]
0	0.000	0.128	0.000
0.06	0.126	0.202	0.212
0.12	0.229	0.314	0.248

for a different number of sensors or a different number of measurement points at the wall of the cavity. In estimations for two and four sensors, it is observed that similar accurate results are obtained, but for one sensor poor estimation is observed. To check the accuracy of the estimations a more exigent test is presented, the estimation of the heat flux on the west wall that uses the intensities calculated near the frontier and near the corners of the cavity. As can be seen in Fig. 6(b), the estimation for two and four sensors is accurate with the exact solution and between them it is close. It can be observed that the estimation for one sensor is very poor.

The rms errors of the inverse solution for four and two sensors are shown in Table 1 and compared with results in [19]. It can be seen that less rms errors are found in this work even when it used only two sensors to obtain measurement intensities. Fig. 7 shows the comparison of the estimation of the heat flux on the west wall using simulated measured exit radiation intensity data for two sensors at different positions at the two appositive vertical walls. Also, σ_o equal to 0.12 is used. It is observed that for the case of symmetrical arrangement more accurate results are found than in the case of non-symmetrical arrangement. Also, in the case of non-symmetrical arrangement, the estimation is less accurate when the sensors are far from the center point of the walls and poor estimations are found when the sensors are near the corners. To examine the influence of the radiative properties on the inverse analysis, simulations for relative errors on the radiative properties were realized. Table 2 shows the effects on the estimations for non-uniform distribution of the absorption coefficient. In simulations two sensors were used. A uniform distribution of radiative properties was used to calculate the exact values, while a non-uniform distribution with 10% random error over a uniform distribution of radiative properties was used to calculate the estimated values (random errors values between −0.05 and 0.05 for the 0.5 value of absorption coefficient). The rms errors of the inverse solution for non-uniform distribution of the absorption coefficient are higher than in uniform distribution, but it can be observed that for σ_o equal to 0.06 and non-uniform absorption distribution the rms error in this work is less than the rms error in [19]. The rms error for σ_o equal to 0.12 and non-uniform absorption distribution can still be considered acceptable.

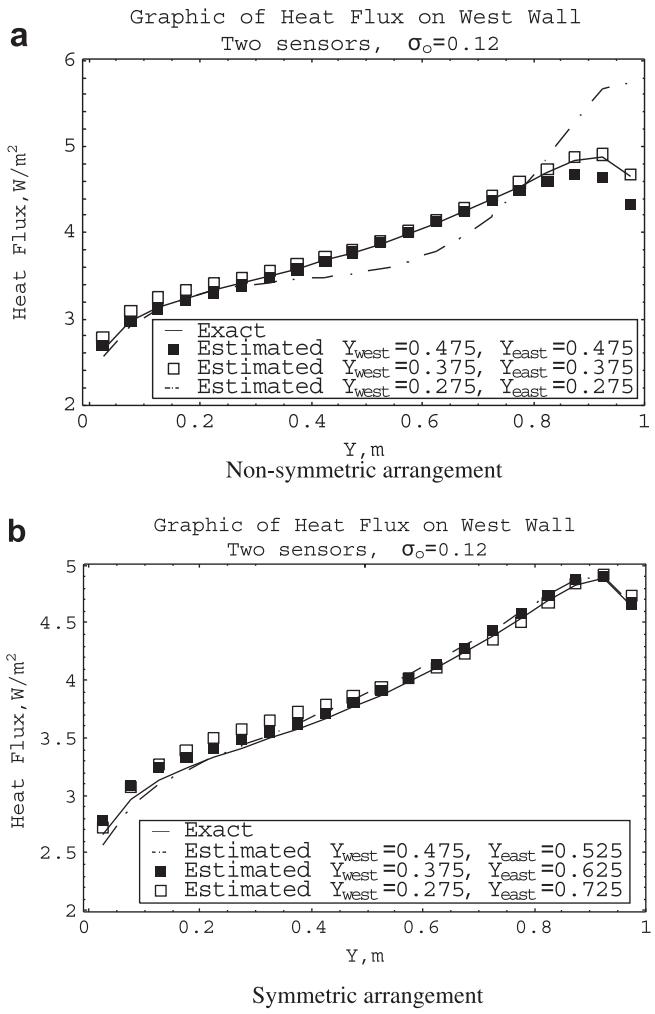

Fig. 7. Comparison of the estimation of the heat flux using simulated measured exit radiation intensity data for two sensors at different positions, for $\sigma_o = 0.12$.

4. Conclusions

An inverse method is presented for estimation of the temperature distribution for a gray emitting, scattering, two-dimensional rectangular medium. The exit radiation intensities at the center of the bounding surfaces are assumed to be known. The direct and sensitive problems are solved using a high order multidimensional scheme for spatial discretization and the LC11 angular quadrature with 60 directions. The inverse problem is solved by using the conjugate gradient method. Noisy input data have been used to test the accuracy of the method used. The results show that the temperature profile can be estimated accurately even with noise data for a high order angular quadrature Tn6 or LC11 in DOM. However the problem is more sensitive to noise data when a lower order of angular quadratures like S_6 or S_4 is used. The results show that the temperature profile can be estimated accurately when the exit radiation intensities at the center of two or four of the bounding surfaces are assumed to be known even with noise data for a high order angular quadrature Tn6 or LC11 in DOM. But the estimations of the temperature profile when the exit radiation intensities at the center of one of the bounding surfaces are assumed to be known are poor. Different arrangements for the sensors position are tested in the case of two sensors and it was found that the temperature profile can be estimated accurately when symmetrical arrangement is used even at the position of the sensors far from the center point of the walls. The results are more sensitive at the position for non-symmetrical arrangement and poor results were found at a position of the sensors far from the center point of the walls.

Acknowledgements

The first author wishes to thank FAPESP for financial support of the young researcher in process 03/12456-7.

References

[1] N.J. McCormick, A critique of inverse solutions to slab geometry transport problems, Prog. Nucl. Energy 8 (1981) 235–245.
[2] N.J. McCormick, Recent developments in inverse scattering transport method, Transp. Theory Stat. Phys. 13 (1984) 15–28.
[3] N.J. McCormick, Methods for solving inverse problems for radiation transport – an update, Transp. Theory Stat. Phys. 15 (1986) 759–772.
[4] N.J. McCormick, Inverse radiative transfer problems: a review, Nucl. Sci. Eng. 112 (1992) 185–198.
[5] H. Ertürk, O.A. Ezekoye, J.R. Howell, Comparison of three regularized solution techniques in a three-dimensional inverse radiation problem, J. Quant. Spectrosc. Radiat. Transf. 73 (2002) 307–316.
[6] F.R. França, J.R. Howell, O.A. Ezekoye, J.C. Morales, Inverse design of thermal systems, in: J.P. Hartnett, T.F. Irvine (Eds.), Advances in Heat Transfer, vol. 36, 2002, pp. 1–110.
[7] K.J. Daun, J.R. Howell, Inverse design methods for radiative transfer systems, J. Quant. Spectrosc. Radiat. Transf. 93 (2005) 43–60.
[8] H.Y. Li, M.N. Ozisik, Identification of temperature profile in an absorbing emitting and isotropically scattering medium by inverse analysis, J. Heat Transf. 114 (1992) 1060–1063.
[9] H.Y. Li, M.N. Ozisik, Inverse radiation problem for simultaneous estimation of temperature profile and surface reflectivity, J. Thermophys. Heat Transf. 7 (1993) 88–93.
[10] A.J.S. Neto, M.N. Ozisik, An inverse problem of simultaneous estimation of radiation phase function, albedo and optical thickness, J. Quant. Spectrosc. Radiat. Transf. 53 (1995) 397–409.
[11] H.C. Yi, R. Sanchez, N.J. McCormick, Bioluminescence estimation from ocean in situ irradiances, Appl. Opt. 31 (1992) 822–830.
[12] C.E. Siewert, An inverse source problem in radiative transfer, J. Quant. Spectrosc. Radiat. Transf. 50 (1993) 603–609.
[13] C.E. Siewert, A radiative transfer inverse-source problem for a sphere, J. Quant. Spectrosc. Radiat. Transf. 52 (1994) 157–160.
[14] L.H. Liu, H.P. Tan, Q.Z. Yu, Inverse radiation problem of boundary incident radiation heat flux in semitransparent planar slab with semitransparent boundaries, J. Thermal Sci. 7 (1998) 131–138.
[15] L.H. Liu, H.P. Tan, Q.Z. Yu, Inverse radiation problem in one-dimensional semitransparent plane–parallel media with opaque and specularly reflecting boundaries, J. Quant. Spectrosc. Radiat. Transf. 64 (2000) 395–407.
[16] H.Y. Li, Estimation of the temperature profile in a cylindrical medium by inverse analysis, J. Quant. Spectrosc. Radiat. Transf. 52 (1994) 755–764.
[17] H.Y. Li, An inverse source problem in radiative transfer for spherical media, Numer. Heat Transf. B 31 (1997) 251–260.
[18] L.H. Liu, H.P. Tan, Q.Z. Yu, Simultaneous identification of temperature profile and wall emissivities in semitransparent medium by inverse radiation analysis, Numer. Heat Transf. A 36 (1999) 511–525.
[19] H.Y. Li, Inverse radiation problem in two-dimensional rectangular media, J. Thermophys. Heat Transf. 11 (1997) 556–561.
[20] H.C. Zhou, P. Yuan, F. Sheng, C.G. Zheng, Simultaneous estimation of the profiles of the temperature and the scattering albedo in an absorbing emitting and isotropically scattering medium by inverse analysis, Int. J. Heat Mass Transf. 43 (2000) 4361–4364.
[21] M.N. Ozisik, H.R.B. Orlande, Inverse Heat Transfer, Taylor and Francis, New York, 2000.
[22] A.N. Tikhonov, Inverse problem in heat conduction, J. Eng. Phys. 29 (1975) 816–820.
[23] A. Björck, Numerical Methods for Least Squares Problems, SIAM, Philadelphia, PA, 1996.
[24] R.C. Hansen, Rank Deficient and Discrete Ill-posed Problems: Numerical Aspects of Linear Inversion, SIAM, Philadelphia, PA, 1998.
[25] C.R. Vogel, Computational Methods for Inverse Problems, SIAM, Philadelphia, PA, 2002.
[26] R. Siegel, J.R. Howell, Thermal Radiation Heat Transfer, third ed. Taylor & Francis Ltd., London, 1992.
[27] W.A. Fiveland, Discrete ordinates solutions of the radiative transport equation for rectangular enclosures, Trans. ASME. J. Heat Transf. 106 (1984) 699–706.
[28] K.A.R. Ismail, C.S. Salinas, Application of multidimensional scheme and the discrete ordinate method to radiative heat transfer in a two-dimensional enclosure with diffusely emitting and reflecting boundary walls, J. Quant. Spectrosc. Radiat. Transf. 88 (2004) 407–422.
[29] D. Balsara, Fast and accurate discrete ordinates methods for multidimensional radiative transfer. Part I, basic methods, J. Quant. Spectrosc. Radiat. Transf. 69 (2001) 671–707.
[30] F.S. Beckman, The solution of linear systems by conjugate gradient method, in: A. Ralston, H.S. Wilf (Eds.), Mathematical Methods for Digital Computers, Wiley, New York, 1960, pp. 62–72.
[31] O.M. Alifanov, Solution of an inverse problem of heat conduction by iteration methods, J. Eng. Phys. 26 (1974) 471–476.
[32] R. Koch, R. Becker, Evaluation of quadrature schemes for the discrete ordinates method, J. Quant. Spectrosc. Radiat. Transf. 84 (2004) 423–435.
[33] C.P. Thurgood, A. Pollard, H.A. Becker, The T_N quadrature set for the discrete ordinates method, J. Heat Transf. 117 (1995) 1068–1070.
[34] H.S. Li, G. Flamant, J.D. Lu, An alternative discrete ordinate scheme for collimated irradiation problems, Int. Commun. Heat Mass Transf. 30 (2003) 61–67.